

The effect of doping process on the structural and optical properties of Ag₂Se thin films.

Cite as: AIP Conference Proceedings **2307**, 020034 (2020); <https://doi.org/10.1063/5.0033127>
Published Online: 15 December 2020

Rana Gamal Mazban, and Iman Hameed Khudayer



View Online



Export Citation

ARTICLES YOU MAY BE INTERESTED IN

[Studying the effect of the annealing on Ag₂Se thin film](#)

AIP Conference Proceedings **2307**, 020007 (2020); <https://doi.org/10.1063/5.0032986>

[Study the effect of heat treatment and pressure on some of the structural properties and electrical conductivity for the nano carbon Nylon66](#)

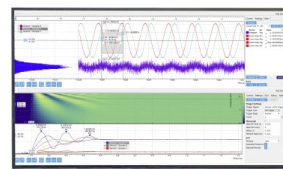
AIP Conference Proceedings **2307**, 020035 (2020); <https://doi.org/10.1063/5.0032936>

[From the architectural acoustic design to measurements: The Auditorium Arvedi case study](#)

AIP Conference Proceedings **2307**, 020036 (2020); <https://doi.org/10.1063/5.0032655>

Challenge us.

What are your needs for periodic signal detection?



Zurich
Instruments



The Effect of Doping Process on the Structural and Optical Properties of Ag₂Se Thin Films.

Rana Gamal Mazban, Iman Hameed Khudayer

Department of Physics, College of Education for Pure Science (Ibn Al-Haitham), University of Baghdad, Iraq.

Abstract. Ag₂Se alloys have been prepared, thin films of this compound has been deposited by the thermal evaporation method under a vacuum of 10⁻⁵ Torr, on coring glass substrate at room temperature. They have a thickness of (500±10) nm and rate of deposition (2.07813nm Sec⁻¹). The Ag₂Se films has been doped by different elements (Al, Bi, Sb, and Cd) with a constant ratio 2% by thermal diffusion method. The structure of the alloys and the thin films have been examined by the XRD method show that the thin films have (Orthorhombic) structure, the doping of all the elements in general caused to conform the crystalline nature and the preferred orientation at (002), with the gain in the crystalline size. The optical properties of the prepared films have been investigated. The optical absorption coefficient (α) of the films was determined from absorbance spectra in the range of wavelength (200-1100) nm. The optical energy gap was found to allow direct transition, which decreases with the doping process, also the optical constant have been calculated. The grain size and roughness have been measured with AFM, they increased by adding impurity element.

Keywords: Ag₂Se thin films, thermal evaporation, doping elements, AFM.

INTRODUCTION

Silver selenide (Ag₂Se) is an (A₂B^{IV} group) narrow bandgap semiconductor with promising thermoelectric properties. Its molar mass is 294.7 g/mol & density 8.216 g/cm³, large magnetoresistance and high electrical conductivity, is a mixed ionic conductor with high concentration [1]. The binary chalcogenide semiconductors have been shown size-dependent optical properties due to quantum size effects. It has a numerous application in nonlinear optical devices and switching devices [2], electrochemical potential memory devices [3], Schottky barrier [4]. the photodetector, solar energy conversion, switching devices, superionic conductor [5], magnetic field sensing device, Infrared sensors, photolithographic layer electrochemical storage cells, semiconducting optical devices for visible region. The crystalline structure has a orth

To date, Ag₂Se has been prepared by various methods, such as hydrothermal, co-precipitation, sol-gel, sonochemical, deposited by vacuum evaporation, solid vapor phase reaction and chemical bath deposition and heating the mixture of the Ag and Se at high temperature [6].

EXPERIMENTAL

Ag₂Se alloys were prepared from their elements (Ag and Se) with 99.999% purity. The weight percentage equal to 2.1961 gm for Ag and 0.803gm for the Se element. Then they mixed well with each other in clean quartz tubes. Under 10⁻³ Torr vacuum the tubes were sealed. The tubes were placed in electric furnace after placing them into containers. The temperature was increased in steps until reaching 1000 C, with a rate of 5C/min where the samples stayed in it for 5h. The ingots were taken out from tubes and powdered very well to usage for preparing thin films on cleaning glass substrates at room temperature. by the thermal evaporation method under a vacuum of 10⁻⁵ Torr. They have a thickness of (500±10) nm and rate of deposition (2.07813nm Sec⁻¹).

The Ag₂Se films has been doped by different elements (Al, Bi, Sb, and Cd) with a constant ratio (2%) of weight by thermal diffusion method, by depositing the doping element on the Ag₂Se films, after calculating the atomic percentages, and then the samples have been putting in electric furnace at 100 C, for one hour.

The thickness (t) of all prepared films was measured by using the weighing method according to the following relation [7]:

$$t = m / A \cdot \rho \dots\dots\dots (1)$$

Where; m, ρ, A were the mass, density and area of the films respectively. Its done by using a sensitive balance whose sensitivity of the order (10⁻⁴) gm.

The crystal structure of the alloy and films was characterized by using X-ray diffraction (XRD) by (Shimadzu6000 X-ray Diffraction) with the copper target of the wavelength (λ=1. 5406) Å. Lattice constants, crystalline size were specified, the inter planar spacing d_{hkl} (Å) between consecutive parallel planes was measured by Bragg's law [8]:

$$n \lambda = 2\theta d_{hkl} \sin(\theta) \dots\dots\dots (2)$$

Where, n is the order of diffraction and θ is the angle of incidence. The average crystalline size can be estimated using the Scherrer's Formula [9]:

$$C.S = \frac{0.94\lambda_{X-Ray}}{\beta_{(FWHM)} \cos \theta_B} \dots\dots\dots (3)$$

Where, β is the full width at half maximum intensity in radians.

The microstrain (ε) developed in the thin films was calculated using the formula [10]:

$$\epsilon = \beta \cos \theta / 4 \dots\dots\dots (4)$$

The dislocation density (δ) was determined for all the thin films using the equation [10]:

$$\delta = 1/D^2 \dots\dots\dots (5)$$

The number of crystallines /unit area can be obtained using the relation [10]:

$$N = t/D^3 \dots\dots\dots (6)$$

(AFM) was employed to investigate the surface morphology of the AgInSe₂ films as a device type of (SPM - AAA3000 contact mode spectrometer, Angstrom). Optical measurement has been constructed using UV-Visible 1800 spectrophotometer.

A spectrophotometer model (UV-Visible 2601) double-beam spectrophotometer is used to measure the absorbance spectrum in the range (200-1100) nm region.

The reflectance calculated from the relation [11]:

$$R = 1 - A - T \dots\dots\dots (7)$$

Where T could be calculated from [12]:

$$T = e^{-2.303A} \dots\dots\dots (8)$$

The optical absorption spectrum was utilized to define the optical energy gap (E_g^{opt}) eV using Tauc formula [13]:

$$\alpha h\nu = B (h\nu - E_g^{opt})^{1/r} \dots\dots\dots (9)$$

Where, B is a constant, hν is the photon energy (eV) and r is constant, that it may take values 2, 3, 1/2, 3/2 depending on the material and the type of the optical transition. The ability of a material to absorb light is measured by its absorption coefficient and it is a very strong role of the photon energy and band gap energy, the absorption coefficient (α) value can be computed from the formula [14]:

$$\alpha = 2.303 \frac{A}{t} \dots\dots\dots (10)$$

Where, A is the optical absorbance.

The optical constants fully express the optical behavior of materials; they are important fundamental properties of matter [15].

The refractive index value can be calculated from the formula [15]:

$$n_o = \left[\frac{4R}{(1-R)^2} - k^2 \right]^{\frac{1}{2}} + \left(\frac{1+R}{1-R} \right) \dots\dots\dots (11)$$

where k represents the extinction coefficient, which is calculated by the relation [16]:

$$k = \frac{\alpha\lambda}{4\pi} \dots\dots\dots(12)$$

The real ϵ_r and imaginary ϵ_i part of dielectric constant can be calculated by using the following equations [17]:

$$\epsilon = \epsilon_r - i\epsilon_i \dots\dots\dots(13)$$

$$\epsilon_r = n_0^2 - k_0^2 \dots\dots\dots(14)$$

$$\epsilon_i = 2n_0k_0 \dots\dots\dots(15)$$

There were many methods for doping semiconductor such that; Mixture Method, Co –evaporation, Laser, Solubility In Solution and Thermal Diffusion method [18].

In this work we use the last one method.

III. RESULT AND DISCUSSION:

Figure (1) displays the X-ray diffraction spectra of Ag₂Se alloys . From this figure we can notice that the spectrum adopts five high polycrystalline peaks equivalent to reflection from (122),(014),(013),(121), and (122) planes of (Orthorhombic) phase.

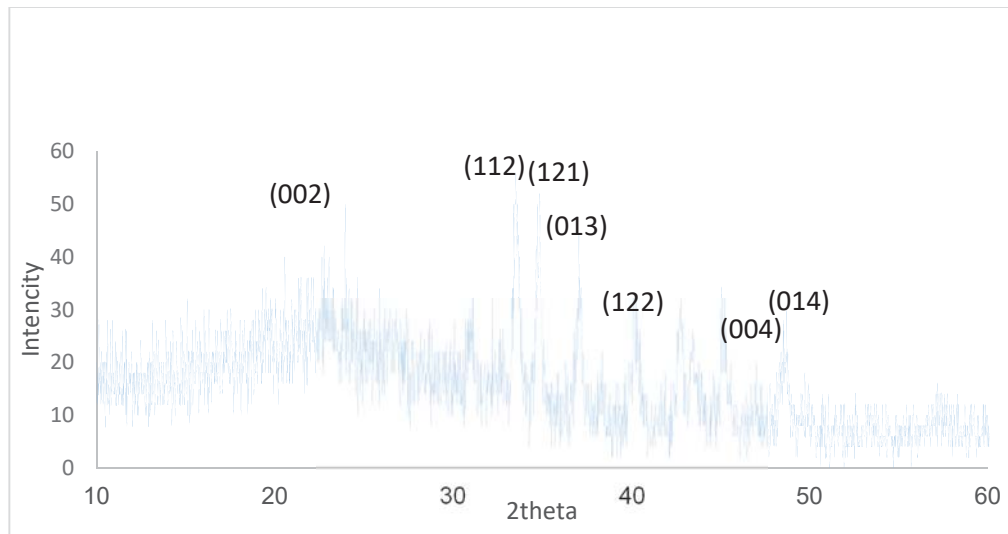


FIGURE 1. XRD spectra of Ag₂Se alloys.

We can see the lattice parameter for Ag₂Se in Table (1):

TABLE 1. XRD parameters of Ag₂Se alloys.

2θ (Std.) (Deg.)	2θ (Exp.) (Deg.)	d _{hkl} (Std.) (Å)	d _{hkl} (Exp.) (Å)	hkl	FWHM (Deg.)	C.S (nm)	a(Std.) (Å)	a(cal.) (Å)
33.49	33.52	2.67	2.67	(112)				
34.86	34.86	2.58	2.58	(121)	0.31000	177	a=4.333 b=7.062 c=7.764	a=4.333 b=7.062 c=7.764
36.97	37.06	2.42	2.42	(013)				
40.2	40.2	2.23	2.23	(122)				
48.5	48.5	1.87	1.87	(014)				

The XRD pattern of Ag₂Se films show that it has polycrystalline structure of (orthorhombic) type, as show in fig.(2). it has preferred orientation at (013). The presented of the broad peak indicted that the films have Nano-structure.

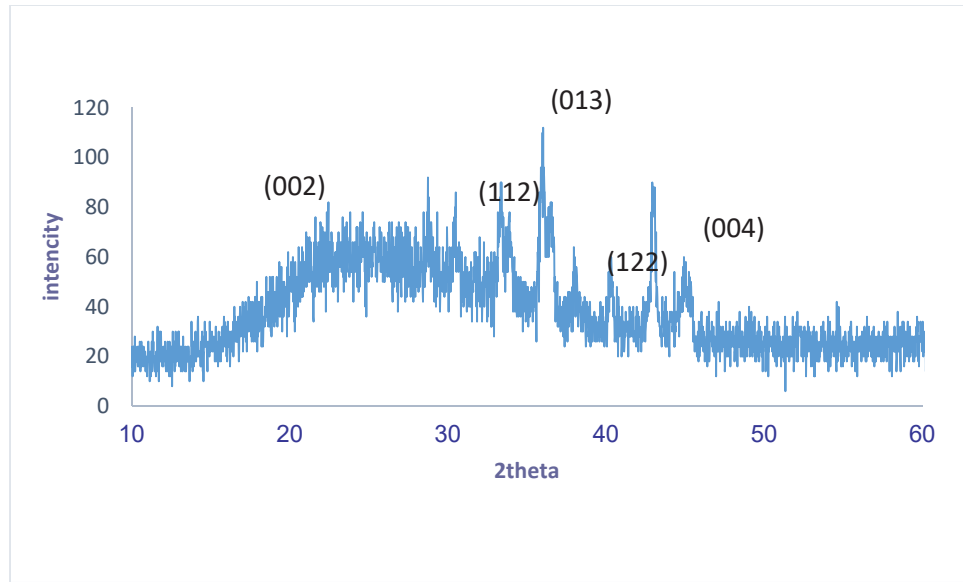


FIGURE 2. XRD pattern of Ag₂Se thin films.

When we compared the results with the standard values in the card (ICDD 00-024-104) we get the following table:

TABLE 2. presented the measured and standard values of XRD parameters for Ag₂Se thin films

2θ (Std.) (Deg.)	2θ (Exp.) (Deg.)	d _{hkl} (Std.) (Å)	d _{hkl} (Exp.) (Å)	hkl	FWHM (Deg.)	C.S (nm)	a(Std.) (Å)
22.919	23.37	3.8	3.8	(002)			
33.43	33.34	2.67	2.67	(112)			
36.9	36.2	2.4	2.4	(013)	0.9500	50	a=4.33 b=7.062 c=7.764
40.2	40.2	2.23	2.23	(122)			

When we use doping with different elements (Al, Sb, Cd and Bi) with constant ratio (2%), the XRD examined show that, there was an conform in the crystalline nature in general, as show in the figure(3).

From fig.(3) the structure of orthorhombic one, the preferred orientation at (002) at two theta equal to 22°. We notice that for Al elements, the intensity has a minimum values because the crystalline nature is small, and it increase for other elements, the better case with Cd. It increases from 120 for pure samples to 2000, 7000, 13000 and 23000 for Al, Bi, Sb and Cd respectively. The reasons for increasing the intensity with the doping process, the atoms of impurities caused to make an atomic localized state in the host material, and this cause that the atoms levels of the both materials will not have scattered the incident x-ray radiation, and this caused a constructive interference which means that there was conform in the crystalline structure.

From the figure it appears that the diffraction angle shifts to smaller values, such that it's equal in pure sample to 36.2, while it becomes 22.8375, 22.6519, 22.7577 and 22.7409 for Al, Bi, Sb and Cd respectively. This due to the variation in the purity and the increase in the crystal size as illustrated in Table (4).

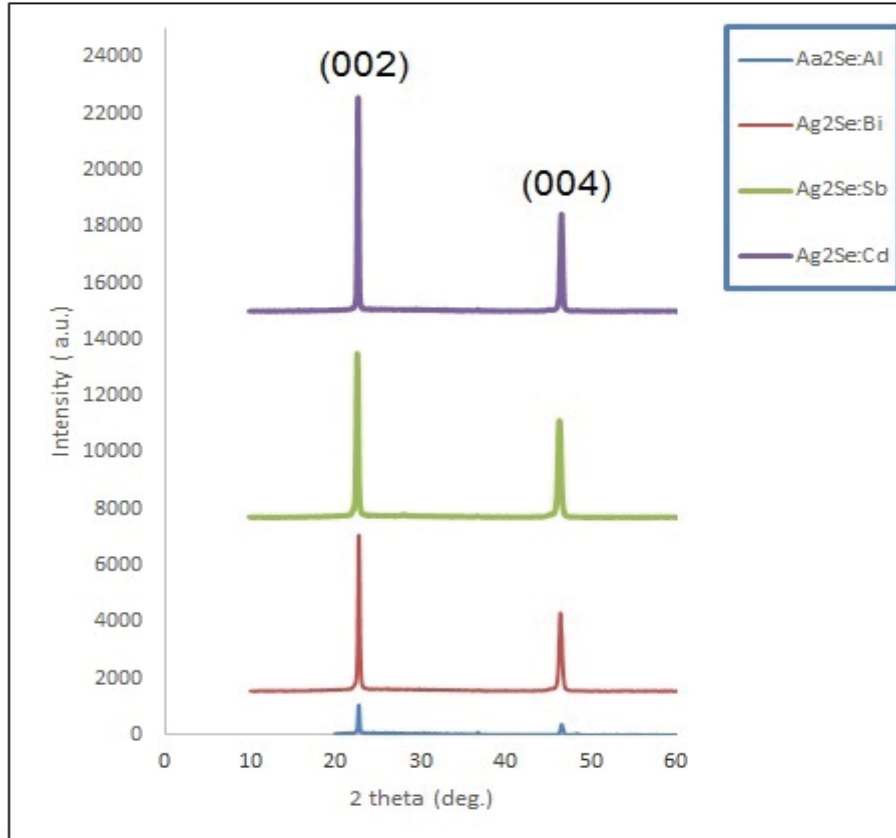


FIGURE 3. The XRD pattern of doped Ag₂Se thin films with different element.

TABLE 3. the XRD parameter of pure and doping films with different elements(Al, Bi, Sb, and Cd).

samples	2 θ (Std.) (Deg.)	2 θ (Exp.) (Deg.)	d _{hkl} (Std.) (Å)	d _{hkl} (Exp.) (Å)	FWHM (Deg.)	C.S. nm	hkl
Ag ₂ Se	36.2	36.2	2.4	2.4	0.17250	50	(013)
Ag ₂ Se:Al	22.8375	22.8375	3.89083	3.89083	0.19970	42.3	(002)
Ag ₂ Se:Bi	22.6519	22.6519	3.90430	3.90430	0.23450	36	(002)
Ag ₂ Se:Sb	22.7577	22.7577	3.92229	3.92229	0.21980	38.5	(002)
Ag ₂ Se:Cd	22.7409	22.7409	3.90714	3.90714	0.17730	47.7	(002)

This increasing value due to the interstitial diffusion; that the size of the parent samples greater than the impurities one as show in Table(5), which presented the crystalline and ionic radii of the impurity atoms; that it's smaller than the host atoms, and this causes to increase its size.

TABLE 4. the crystalline, ionic radii of host and doping elements.

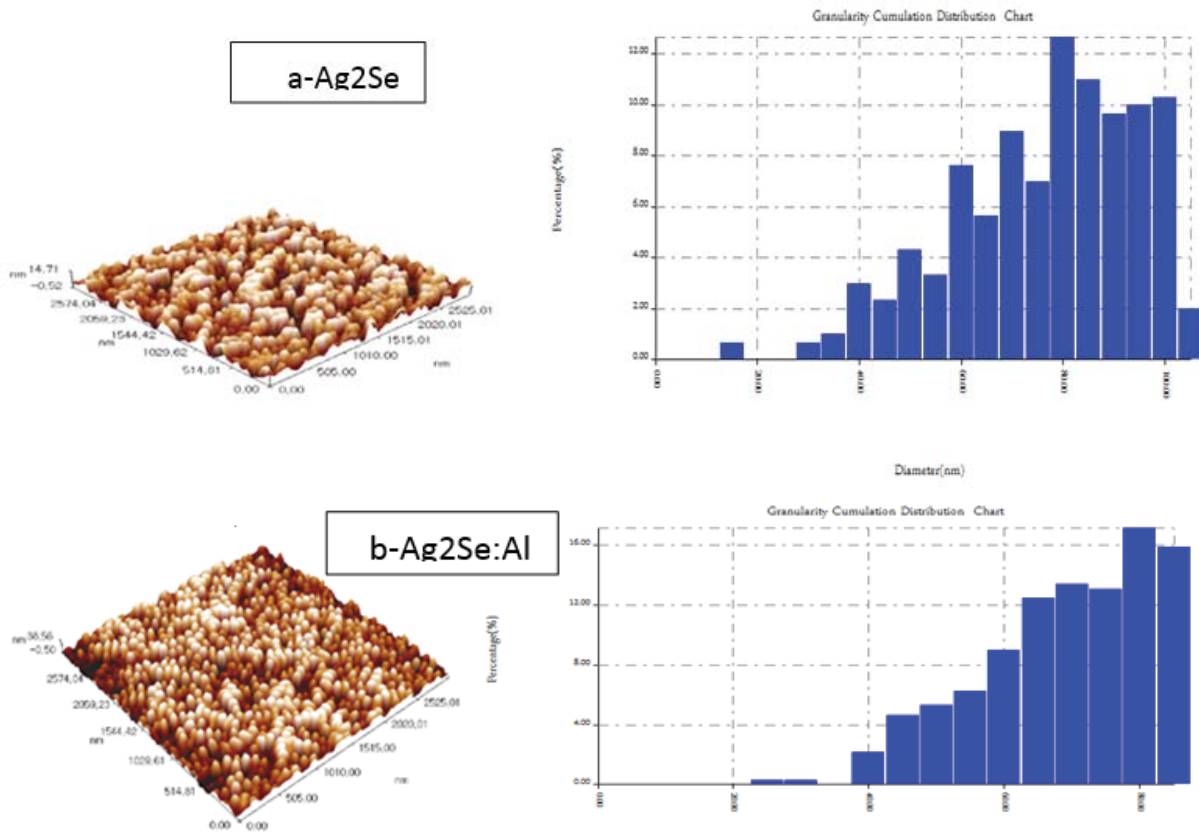
Samples	CR(Å) [19]	IR(Å) [19]
Ag ₂ Se	0.93	0.79
Al ⁺³	0.67	0.53
Sb+3	0.9	0.76
Sb+5	0.76	0.6
Bi+3	1.17	1.03
Bi+5	0.9	0.76
Cd+2	1.09	0.95

The micro strain, dislocation density and number of crystalline/area also have been calculated using equations (4), (5) and (6) respectively, which also increase with the doping process as shown below table. The dislocation increase due to the increase of crystal size, as mention above as the doping cause to increase the crystal constant, due to the microstrain, and this in turn resulted from the vibration of the ion radii, as indicated in table (5), which depending on the charge states and on the spin states of the magnetic ions.

TABLE 5. Strain parameters of the host and impurity atoms.

sample	C.S (nm)	Microstrain	(N) x1015 (per m2)	(δ)x1014 (per m2)
Ag2Se	50	0.04	2	4
Ag2Se:Al	42.3	0.048	2.7	5.5
Ag2Se:Sb	38.5	0.053	3.3	6.7
Ag2Se:Bi	36	0.057	3.8	7.7
Ag2Se:Cd	47.7	0.05	2.1	4.3

Figures (4) and its parties display the 2D and 3D AFM images of all thin Ag2Se films before and after doping, which confirms that all films adopt dense and homogeneous surfaces with spherical like shape particles. This result confirms the fact which estimated from XRD examine of enhancement the crystalline structure by doping.



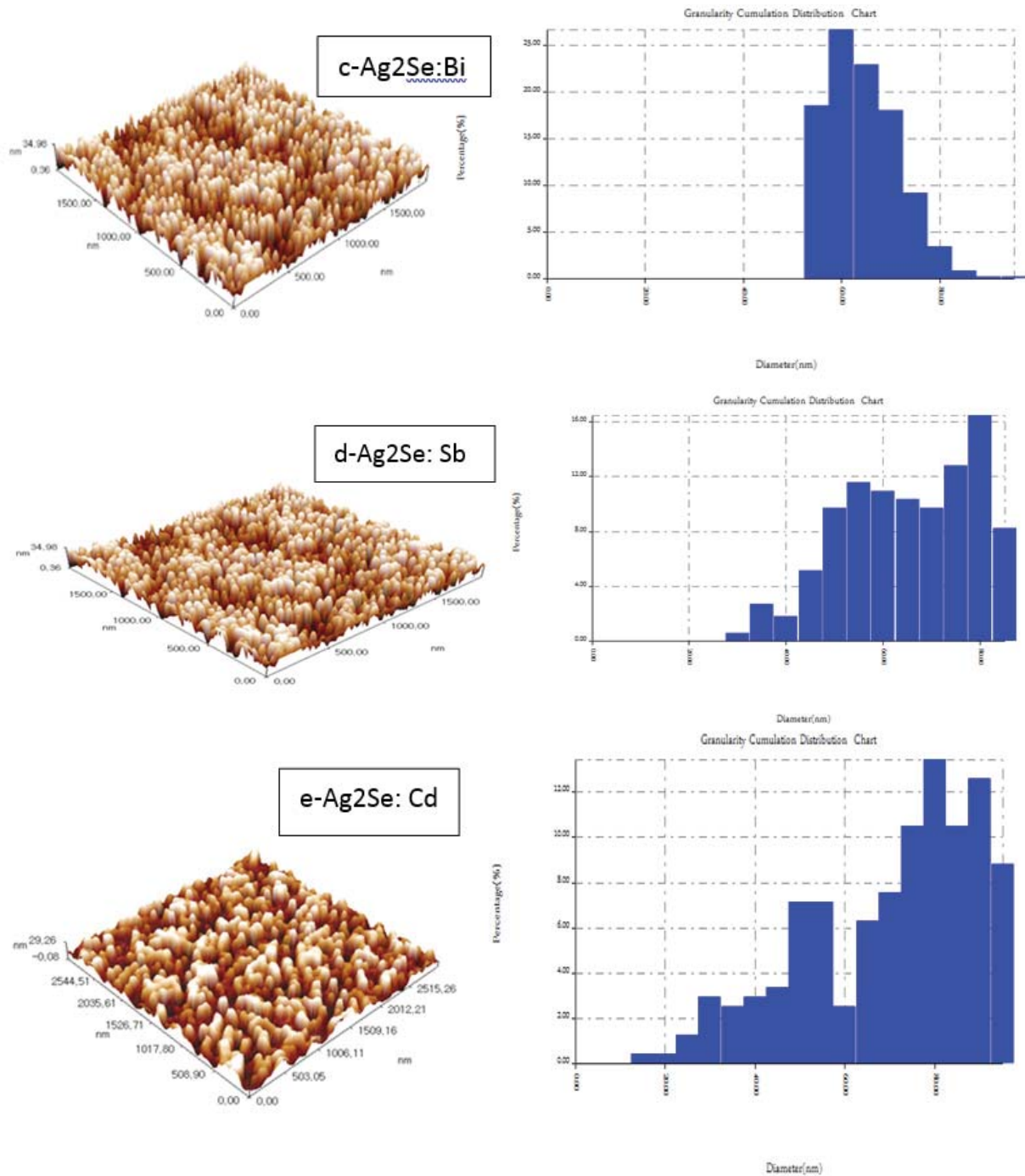


FIGURE 4. The 2D and 3D AFM images of Ag₂Se films and doped with different elements.

The grain size and roughness increase as show in table (7), it can be noticed that these parameters increase with doping. The increase in grain size greater than the C.S which estimated from XRD analysis and indicates that impurities atoms work as a flux which helps in growth of grains [20]. Large grain size causes the decrease of grain boundaries so, the centers of trapping electrons will decrease, and therefore the large grain size is very beneficial for solar cell application [21, 22].

TABLE 6. The average grain size, roughness and r.m.s of pure Ag₂Se thin films and doped with different elements (Al, Sb, Bi and Cd).

Thin film	Grain Size(nm)	Roughness Average(nm)	R.m.s (nm)
Ag ₂ Se	74.06	3.81	4.4
Ag ₂ Se:Al	66.68	7.33	8.47
Ag ₂ Se:Sb	62	8.82	10.2
Ag ₂ Se:Bi	61	8.66	9.99
Ag ₂ Se:Cd	67.85	9.73	11.2

The optical properties have been investigated of pure Ag₂Se thin films and doped one.

The measured absorption spectra for all the samples in the range (200-1100) nm illustrated in fig. (7).

The absorption has a great value in the visible range (300-600) nm, and the peaks at 450 nm than it becomes to drops to small values in the IR region, begins from 650 to 1100 nm, which that the films has good application to solar cell.

As the films become doping, the absorption in general decrease, due to increase the crystal size and conform the crystalline structure as mentioned before. As the size increase there was a shifting of absorption spectra to IR region due to quantum size. The absorption coefficient plotted as a function of wavelength, presented in fig.(8) . It has the same behavior like the absorption values.

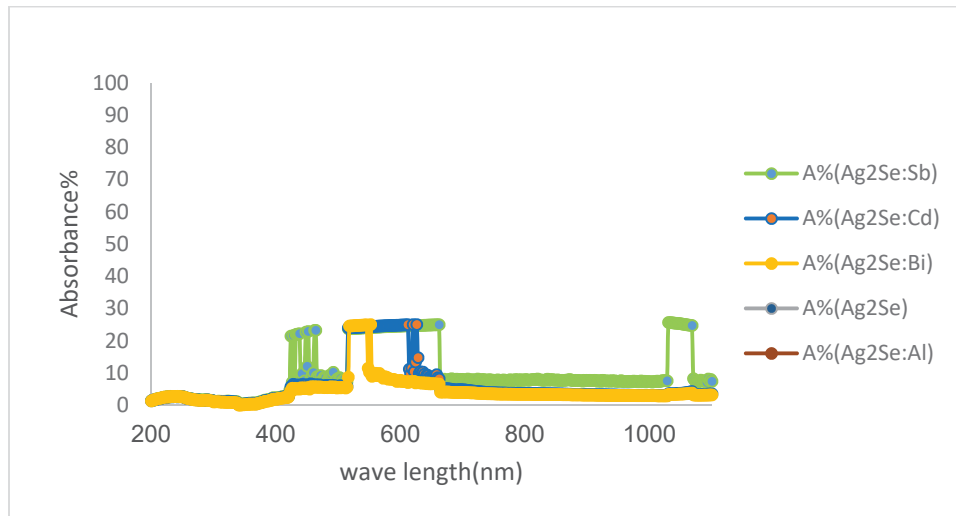


FIGURE 5. The absorption spectrum of pure and doped thin films.

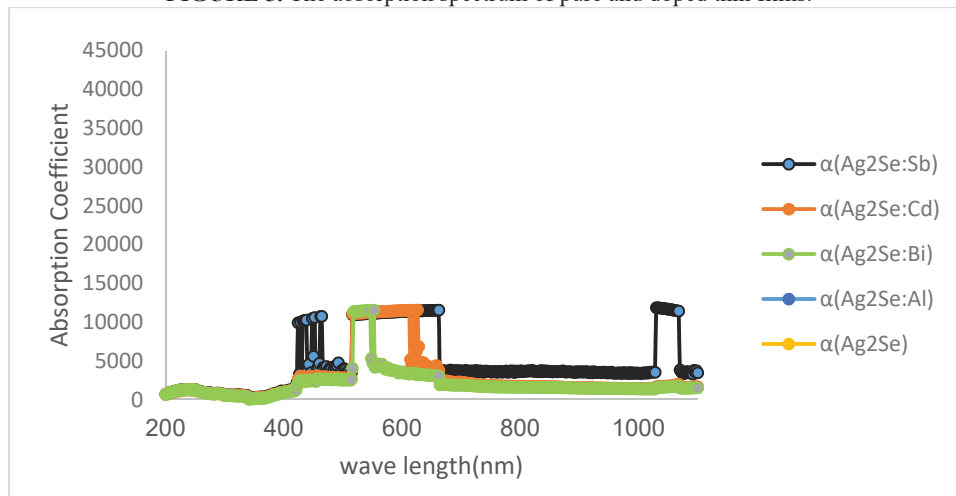


FIGURE 6. The variation of absorption coefficient with doping.

The optical energy gap decrease in doping such that it's equal to; (2, 1.9, 1.65, 1.7 and 1.8) eV for Ag₂Se, doped Al, Bi, Sb and Cd respectively.

This drop due to the generated localized state of the impurity elements, near the conduction or valance band causing the decreasing of the energy gap, this state has little ionization energy depending on the ion radii, which listed in the table (5).

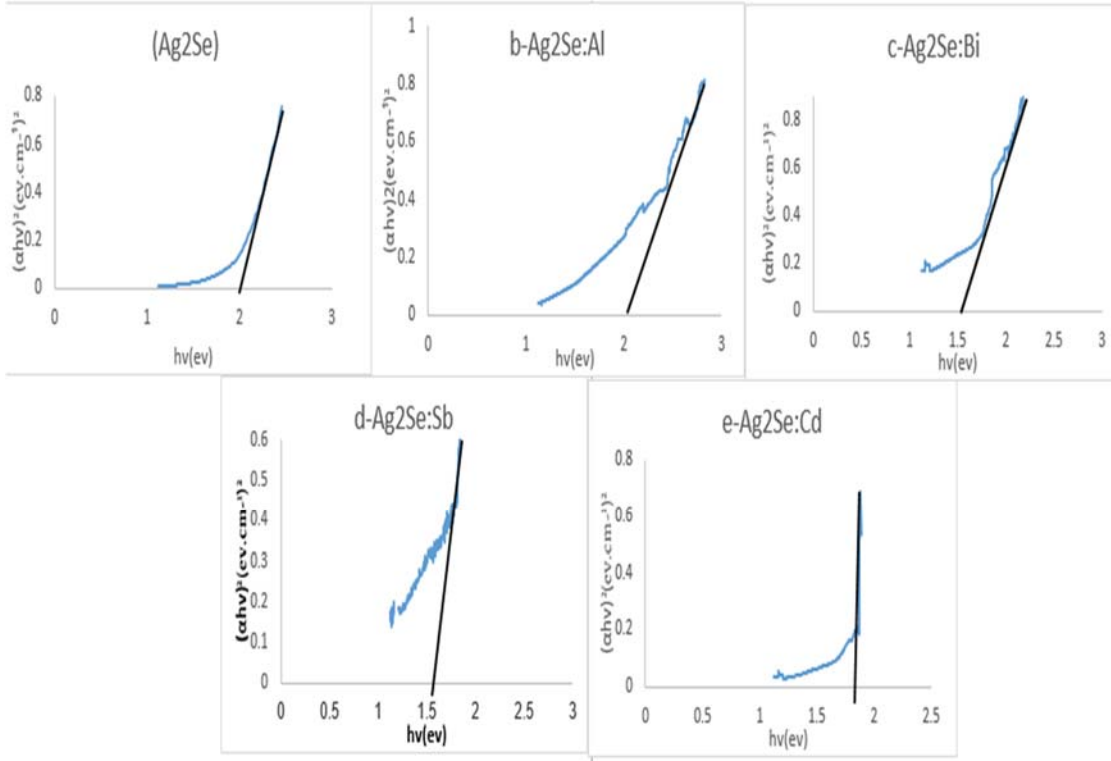


FIGURE 7. The variation of optical energy gap with doping.

The optical parameters that calculated from equations (9-14), their values deduced at 500 nm wavelength, presented in Table (8).

The reflection increase in general in doping because of the increase in roughness, especially in the case of Al, due to its metallic properties. While the refractive index increase in general due to the gain in reflection values. The behavior of extinction coefficient; as illustrated in the table; it falls to lower values, as same as the absorption coefficient behavior.

As for the dielectric constant; the real part increase like the refractive index. In addition the imaginary one fall like extinction coefficient.

TABLE 7. The optical parameters of pure and doped thin films at wave length 500nm.

Optical parameter	Pure and doped thin films.				
	Ag ₂ Se	Ag ₂ Se:Al	Ag ₂ Se:Bi	Ag ₂ Se:Sb	Ag ₂ Se:Cd
T%	16.36641	2.946728	88.04592	84.6747	87.21538
R%	5.028937	58.78677	6.425004	8.100666	6.843929
A%	78.60465	38.2665	5.529077	7.224633	5.940694
k	0.14412930	0.070165406	0.010138108	0.013247077	0.010892848
ε _r	1.287383	2.778084	1.430621	1.287383	1.462157
ε _i	0.329695	0.234104736	0.024252967	0.033088931	0.02634426
n	1.143747	4.206191	1.196129	1.248914	1.209246
α	36205.3	17625.55	2546.693	3327.666	2736.283434

REFERENCES:

1. M C SANTHOSH KUMAR and B PRADEEP, "Electrical properties of silver selenide thin films prepared by reactive evaporation", *Bull. Mater. Sci.*, Vol. 25, No. 5, October 2002, pp. 407–411. © Indian Academy of Sciences.
2. M C Santhosh Kumar and B Pradeep, "Structural, electrical and optical properties of silver selenide thin films", *Semicond. Sci. Technol.* 17 (2002) 261–265.
3. Yuri S. Tveryanovich, Aleksander A. Razumtcev, Timur R. Fazletdinov, Andrey S. Tverjanovich, and Evgenii N. Borisov, "Fabrication of stoichiometric oriented Ag₂Se thin film by laser ablation", *Thin Solid Films* 666 (2018) 172–176.
4. Maryam Jafari, Masoud Salavati-Niasari and Fatemeh Mohandes, "Synthesis and Characterization of Silver Selenide Nanoparticles via a Facile Sonochemical Route Starting from a Novel Inorganic Precursor", *J Inorg Organomet Polym* (2013) 23:357–364
5. Ranjeet Singh¹, Rajesh Kumara, S. K. Sharmab and S. K. Chakarvartiac Department of, "NON-GALVANIC SYNTHESIS OF Ag₂Se NANOWIRES USING ANODIC ALUMINA MEMBRANE AS TEMPLATE AND THEIR CHARACTERIZATION", *Digest Journal of Nanomaterials and Biostructures* Vol. 1, No. 4, December 2006, p. 149 – 154.
6. J. B. Conn and R. C. Taylor, "Thermoelectric and Crystallographic Properties of Ag₂Se", 1960 *J. Electrochem. Soc.* 107 977Thermoelectric
7. O. S. Razzaq, "Fabrication and Study of The Electrical and Photovoltaic Characteristic of CdS/Si Heterojunction", M. Sc. Thesis, College of Education, Al-mustanisiriya University. (2000). and crystallographic Properties of Ag₂Se
8. W. D. Callister "Materials Science and Engineering: An Introduction", John Wiley & Sons, Inc, New York (2007).
9. A. A. Shehab, S. A. Maki and Ayad A. Salih, "The Structural and Surface Morphology Properties of Aluminum Doped CdO Thin Films Prepared by Vacuum Thermal Evaporation Technique", *Ibn Al-Haitham J. for Pure & Applied Science*, 27(2): 158-169, (2014).
10. P.A.Chane, V.D.Bhabad, "Aluminum doped CdSe thin films: structural characterization", *Issue:10, Vol. 2, 2016.*
11. J.I. Pankove, "Optical Processes in Semiconductors", by Prentice Hall, Inc., (1971).
12. B.Saporal and C. Herman, "Physics Of Semiconductors", University of New York, (1995).
13. J.Tauc, "Amorphous and liquid Semiconductors", Plenum press, London, N.Y., (1974).
14. D. A. Neamen, "Semiconductor Physics and Devices", University of New Mexico, (1992).
15. N.A. Subrahmanyam, "A text book of Optics", 9th edition, Delhi India, (1977).
16. K.L.Chopra, "Thin Film Phenomena", McGraw - Hill, New York, (1969).
17. J.C. Phillips, "Bonds and Bonds in Semiconductors", Academic Press, New York and London, (1973).
18. M. G. Yousif, "Solid State Physics", Vol.2, Baghdad University, Arabic Version, (1989).
19. Huheey, James E., et al. *Inorganic chemistry: principles of structure and reactivity.* Pearson Education India, 2006.
20. Kumar M.S., Madhusudanan S. P., Batabyal S. K., "Substitution of Zn in Earth-Abundant Cu₂ZnSn(S,Se)₄ based thin film solar cells-A status review", *Solar Energy Materials and Solar Cells*, 185, (2018), 287-299.
21. Henry J., Mohanraj K., and Sivakumar G., "Photoelectrochemical cell performances of Cu₂ZnSnSe₄ thin films deposited on various conductive substrates", *Vacuum*, 156, (2018), pp. 172-180.
22. Guo H., Ma Ch., Zhang K., Jia X., Li Y., Yuan N., and Ding J., "The fabrication of Cd-free Cu₂ZnSnS₄-Ag₂ZnSnS₄ heterojunction photovoltaic devices" *Solar Energy Materials and Solar Cells*, 178, (2018), 146-153.